MEMS TUNABLE FABRY-PEROT FILTERS WITH THICK, TWO SIDED OPTICAL COATINGS

P. A. Stupar, R. L. Borwick III, J. F. DeNatale, P. H. Kobrin, W. J. Gunning*
Teledyne Scientific and Imaging, Thousand Oaks, CA, USA

ABSTRACT

A MEMS based tunable Fabry-Perot Filter array has been designed and fabricated to provide spectral information in the Long-Wave Infra-Red (LWIR) band, while remaining transparent in the Mid-Wave Infra-Red (MWIR) band. Due to the stringent requirements on the optical design, relatively thick optical reflector and anti-reflector coatings are needed. A two-sided, SOI device layer transfer process has been developed to fabricate the thick coating layers and maintain a balanced stress state on the thin moveable membrane of the filter. Fabricated parts have less than 11 nm of deflection across a 200µm filter. Measured filters show a <120nm bandwidth peak in the LWIR that is tunable from 11.8µm to 7.9µm.

KEYWORDS

MEMS, imaging, tunable filter, Fabry-Perot, spectral imaging

INTRODUCTION

Spectral information can significantly enhance the ability to detect and identify imaged objects [1]. Hyperspectral sensors, with the ability to spectrally resolve an image into tens to hundreds of bands, can enable reliable object discrimination and can also be used to analyze the characteristics of unknown materials. Conventional spectral imaging devices are typically characterized by significant size, weight and data processing penalties, which often limit their utility and applications. To combat these limitations, a new MEMS based Fabry-Perot filter array has been designed and fabricated that can be directly integrated onto an existing focal plane array.

The Adaptive Focal Plane Array (AFPA) is a new spectral imaging technology integrating an array of MEMS tunable filters with a dual-band IR focal plane array. This will provide the ability to acquire spectrally-tuned spatial information in the LWIR while preserving broadband imaging capability in the MWIR. To facilitate this, a MEMS based Fabry-Perot filter array has been designed with broadband transmission in the MWIR 3.5-5.5µm range and a tunable, narrow bandwidth transmission in the LWIR 8-11µm range.

DESIGN

The tunable filter is comprised of an array of MEMS-based Fabry-Perot filters, Fig.1, that provide transmission over a narrow bandwidth, defined by the reflector coatings and the air gap dimension [2]. A two-layer structure is used for the individual filters, comprised of a stationary Si supporting substrate and a movable Si thin membrane. Mechanical motion of the mirror is achieved via electrostatic actuation by applying a potential between the stationary and movable filter elements.

A key challenge is the integration with the multi-layer dielectric coatings, which must be quite thick (13µm of coatings on a 12 µm silicon membrane) to achieve high LWIR filter transmission, narrow bandwidth, and dual-band operation [3]. This can impose significant stresses that can deform the thin movable membrane. In addition, the filter array is designed to operate at 77K, the temperature at which the dual-band FPA has a low enough dark current to function. These optical coating stresses, along with the CTE mismatch deformation caused by cooling the filter array, can degrade filter bandwidth and transmission. Therefore, the stresses must be balanced between the high reflector and AR coatings on both sides of the thin silicon, movable membrane.

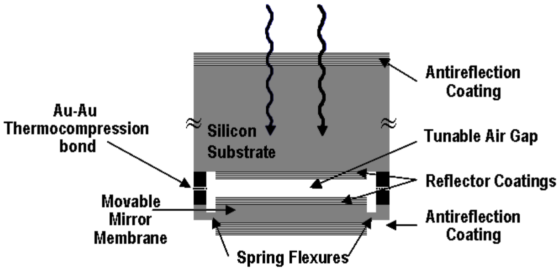

Figure 1. Schematic cross-sectional representation of an individual MEMS tunable filter element.

FABRICATION

The MEMS Fabry Perot filter array is fabricated using an SOI device layer transfer process previously developed for MEMS based sensors [4]. This process was extended to allow processing on all four surfaces of the bonded wafer pair. This is necessary to fabricate a device with the high quality reflective and anti-reflective coatings required for the Fabry-Perot filter.

The two-sided process consists of a processed, SOI device layer that is transferred onto a processed silicon substrate using a Au-Au thermocompression bond (Fig. 2). The high reflectivity coating design requires an 8µm thick multi-layer dielectric stack. To pattern this thick layer, the silicon substrate and SOI wafer are both processed with a 12µm thick PMGI masking layer with a 1µm PECVD oxide top layer. The oxide is patterned using RIE and the PMGI is isotropically etched in an O2 plasma (Fig 2a/d). This creates the necessary undercut of the PMGI layer to successfully lift off of the thick dielectric coatings. The silicon is then etched using DRIE to recess the dielectric coatings to facilitate further processing. The multi-layer, high reflector dielectric is then deposited using E-beam evaporation and lifted off in a heated Microchem 1165 solution. Both wafers are then patterned with gold bonding pads and routing lines (Fig. 2c/e). The SOI wafer is thinned in the area of the mirror suspension using DRIE to reduce the voltage required to actuate the filter (Fig. 2f).

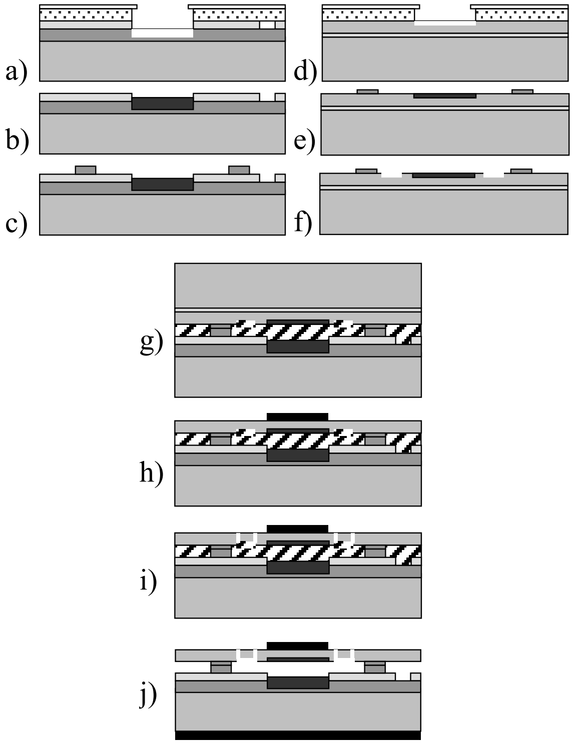

Figure 2. Process flow for a two side coated MEMS Fabry-Perot etalon.

The two wafers are bonded together to form the etalon cavity using a Au-Au thermo-compression bond at 250C and 3000mbar pressure. This is the maximum temperature permitted for the multi-layer dielectric to maintain its optical properties. The bonded wafer is then backfilled with an epoxy layer to provide robustness during the handle wafer removal (Fig. 2g). This epoxy is wicked between the two bonded wafers, fully filling the 6µm gap to the center of a 4 inch wafer. The handle wafer is removed using wafer grinding followed by DRIE to stop on the buried oxide layer.

Using the same PGMI lift off process used for the high reflector, a 5µm thick AR coating is patterned over the movable portion of the mirror (Fig. 2h). Due to the thickness of the dielectric layers and the relative thinness of the silicon device layer, the stress level of the AR coating must be precisely controlled to counteract the stress of the reflector coating and maintain mirror flatness.

The stress of the reflector coating alone will typically create approximately 100nm of deflection across a 200µm filter. Because the AR coating is typically thinner than the reflector coating, it must be deposited with a higher stress level to fully compensate for the deflection caused by the reflector coating. The stress of the AR coating is tailored using the temperature of the e-beam deposition. Using thinned surrogate wafers, the stress of the AR coating is optimized to counteract the deflection caused by the stress of the high reflectivity coating previously deposited. Once the correct AR stress conditions are determined, the coatings are applied to the device wafers.

The silicon device layer is patterned using DRIE to form the suspensions and isolate the individual devices (Fig. 2i). The mirrors are then released using an O_2 plasma to remove the epoxy (Fig. 2j). Figure 3 shows the fabricated filter array. Figure 4 shows the underside of an individual filter with the recessed high reflector coating, the thinned flexure beams and the Au bonding pads.

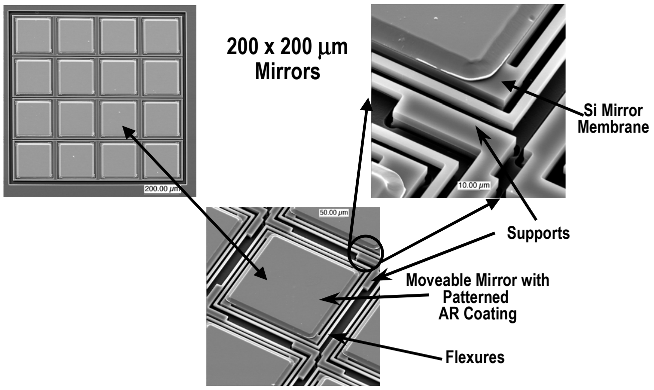

Figure 3. SEM's of the top side of the moveable MEMS mirror.

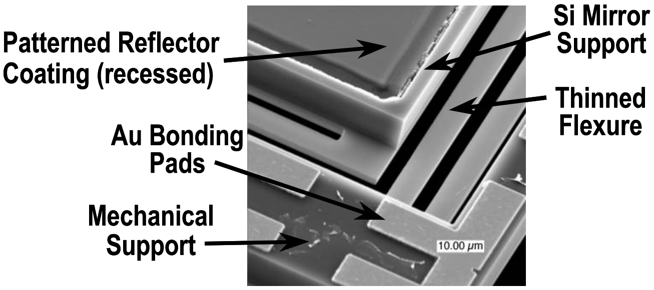

Figure 4. SEM of the bottom side of the moveable MEMS mirror.

RESULTS

Testing of the MEMS Fabry-Perot filters was performed using a variety of different test setups. Mirror flatness was measured using a white light interferometer. As previously discussed, the stress of the two thick dielectric layers must be balanced to maintain the necessary mirror flatness. Using optical simulations, it has been determined that a maximum of 35nm of curvature is acceptable to maintain a filter bandwidth below 120nm. In addition, the device is designed to be operated at the cryogenic temperature required for the long-wave focal plane array. Therefore, the mirror must be fabricated in a pre-stressed state at a curvature that will flatten out as the device is cooled to 77K. Figure 5 shows the curvature of an individual filter measured at room temperature. As shown, the device has an edge to center deflection of 80nm. Figure 6 shows the same filter after cooling the device down to 77K. The CTE mismatch between the optical coatings and the silicon structural layer reduces the curvature of the filter into the noise level of the measurement, less than 10nm.

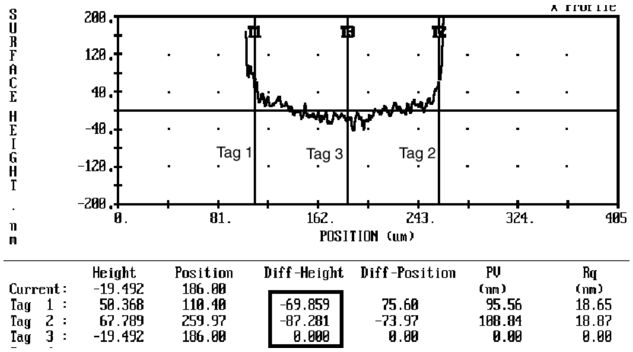

```
           Height    Position   Diff-Height  Diff-Position    PV        Rq
Current:   -19.492   186.00                                  (nm)      (nm)
Tag  1 :    50.368   110.40      -69.859       75.60         95.56     18.65
Tag  2 :    67.789   259.97      -87.281      -73.97        108.84     18.87
Tag  3 :   -19.492   186.00        0.000        0.00          0.00      0.00
```

Figure 5. Curvature of an individual filter measured at room temperature. The edge to center deflection is approximately 80nm. (Diff-Height referenced to Tag T3)

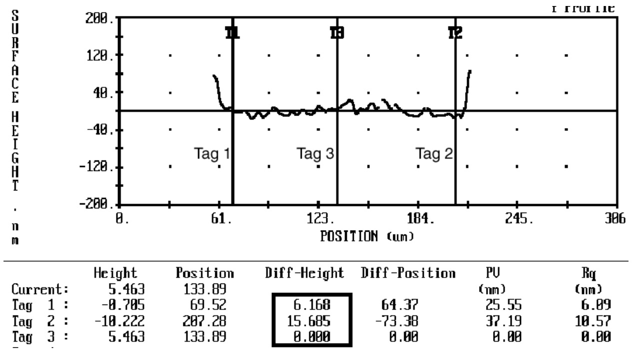

```
           Height    Position   Diff-Height  Diff-Position    PV        Rq
Current:     5.463   133.89                                  (nm)      (nm)
Tag  1 :    -0.705    69.52        6.168       64.37         25.55      6.09
Tag  2 :   -10.222   207.28       15.685      -73.38         37.19     10.57
Tag  3 :     5.463   133.89        0.000        0.00          0.00      0.00
```

Figure 6. Curvature of the filter from figure 5 measured at 77K. The edge to center deflection has been reduced to under 10nm. (Diff-Height referenced to Tag T3)

The filter response and tuning range were measured using an IR microscope. To control and actuate individual filters in the array, the filter array chip is indium bump bonded onto a CMOS control circuit. The control circuit also implements charge control actuation that allows the filers to be tuned to a gap that exceeds the 1/3 gap limit of voltage controlled electrostatic devices [5]. Figure 7 shows the untuned filter spectral response. As shown, the filters are transparent in the MWIR range of 3.5-5.5µm and have a strong narrow transmission peak in the LWIR range.

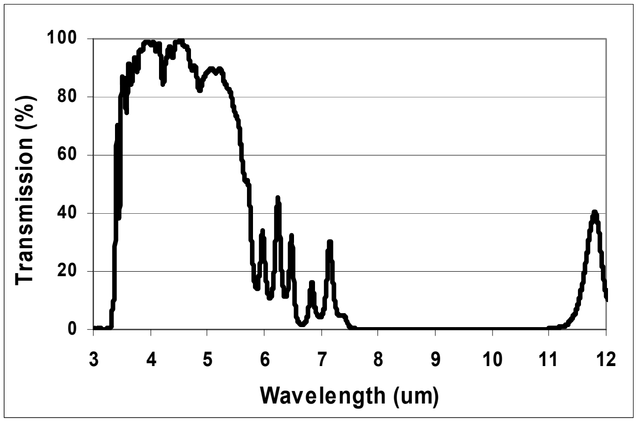

Figure 7. IR transmission spectrum for a single filter device showing the MWIR broadband transmission and a narrow band LWIR transmission at 11.8µm.

Figure 8 shows the room temperature LWIR filter transmission for various control circuit position settings. The LWIR filter transmission can be tuned from 11.8µm to below 8µm. This tuning range is greater than 45% of the initial etalon gap and therefore proves the functionality of the change control circuit. Because the device is intended to operate at 77K, the tuning characteristics were measured using the IR microscope and a dry N2 filled cryogenic chamber. The filter transmission and tuning range is similar to the room temperature results with a 40nm shift toward the long-wave, likely caused by the previously discussed flattening of mirror due to CTE effects.

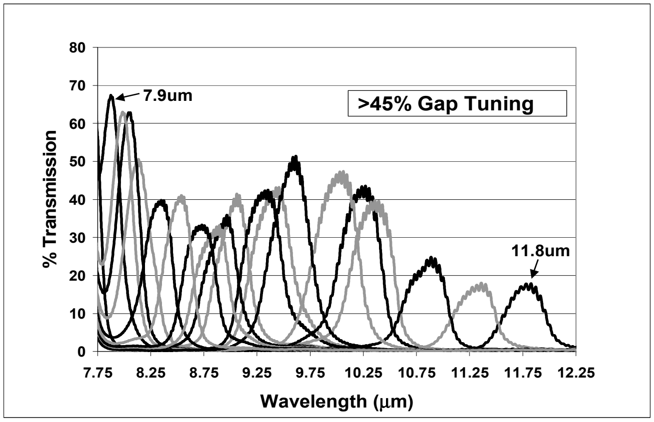

Figure 8. Room temperature LWIR transmission spectrum for a single device at multiple actuation points.

The IR microscope measures transmission using a steep cone angle with an obscured central portion. This optical configuration creates a measurement artifact with significant broadening of the apparent bandwidth. To measure the true bandwidth of the filters, a high f/# tunable CO_2 laser system was used. By tuning the laser to its various lines between 9 and 11 µm and moving the MEMS filter through the laser line, the true filter bandwidth can be measured. Figure 9 shows the filter transmission through six different CO_2 laser lines. As shown the Full Width Half Max (FWHM) filter bandwidth is close to the 120nm design value over the entire range of the device.

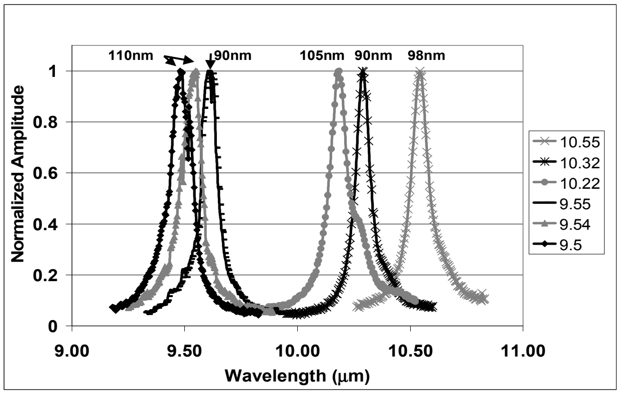

Figure9. LWIR transmission spectrum showing the narrow bandwidth of the tunable filters.

The tunable filter array and control circuit were packaged with a dualband (MWIR / LWIR) focal plane array to test the integrated operation of the device as well as prove the low temperature (77K) performance of the filters (Fig. 10). Filter response was measured using a monochromator that was focused through an individual filter and onto the focal plane array. By tuning the monochromator through the filter line and measuring the FPA response, the filter transmission can be measured. Tuned narrowband spectral response was achieved over the 11.0 – 8.0μm range (Fig. 11).

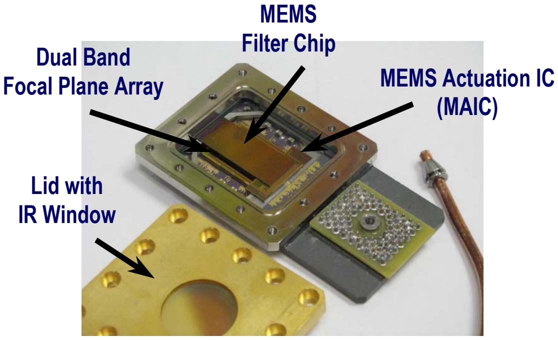

Figure 10. Packaged dual band FPA integrated with an indium bump bonded MEMS tunable filter array and CMOS control circuit.

CONCLUSION

We have designed and fabricatied a MEMS Fabry-Perot filter array that is capable of tuning over a 11.8-7.9μm spectral range while remaining transparent in the 3-5μm range. A robust process was developed to fabricate these devices with precise stress control of the thick-film, multi-layer optical coatings to maintain the flatness needed for the filters to function. These filter arrays were integrated with a CMOS based control circuit and a dual-band focal plane array to show the usefulness of such a device. Future work will concentrate on building prototype systems that enable hyper-spectral LWIR imagery.

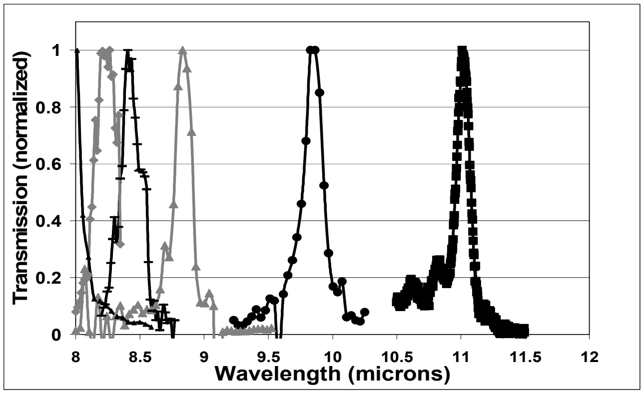

Figure 11. Measured normalized transmission of integrated AFPA device showing tuned narrow band spectral response over the 8 – 11 μm band.

ACKNOWLEDGMENTS

This work was sponsored by DARPA/MTO and under contract from the US Army RDECOM CERDEC Night Vision and Electronic Sensors Directorate. We thank Ray Balcerak and Stuart Horn, DARPA Program Managers, and Joe Pellegrino and Phil Perconti of NVESD for their strong support and guidance in this effort. The authors also acknowledge the efforts of the many Teledyne Scientific and Imaging researchers who contributed to the work described here.

Approved for Public Release - Unlimited Distribution (US Army CECOM Public Affairs Office, 3/30/2009)

REFERENCES

[1] J. Carrano et al, "Tuning in to Detection: Combining Tunability and High Resolution FLIR Detection Improves Target Recognition," OEmagazine, pp. 20-22, April 2004.

[2] M. Born and E. Wolf, *Principals of Optics, Sixth Edition*, Pergamon Press, Oxford, 1980, pp. 323-333

[3] W. Gunning et al, "Dual band focal plane array: An example of the challenge and potential of intelligent integrated microsystems." SPIE Proceedings, vol. 6232, pp. 62320F, 2006

[4] R. Borwick et al, "A high Q, large tuning range MEMS capacitor for RF filter systems," Sensors and Actuators A, Vol. 103, pp. 33-41, 2003

[5] J. Seeger et al, "Charge control of parallel-plate, electrostatic actuators and the tip-in instability," J. Microelectromech Syst., Vol. 12, No 5, pp. 656-671, 2003

CONTACT

* Philip Stupar, tel: 805-373-4926: pstupar@teledyne.com